NUMERICAL ANALYSIS OF DAMAGED PILES DUE TO SOIL LIQUEFACTION DURING HYOGOKEN-NANBU EARTHQUAKE

S. FUJII, H. FUNAHARA and J. YAMAGUCHI

Technology Research Center, Taisei Corporation,
344-1 Nasemachi, Totsuka-ku, Yokohama, Japan

ABSTRACT

During the 1995 Hyogoken-Nanbu Earthquake, Japan, of magnitude 7.2, widespread liquefaction was observed on reclaimed land. A numerical simulation of the soil liquefaction and the response of a building which suffered a damage to its piles, was conducted. Two numerical methods are employed. The first method is an effective stress finite element analysis of a soil-pile-building system. The finite element code DIANA-J with the Stress-Density Model (S-D Model) as a constitutive model is used. The ground liquefaction, the resulting large ground displacement, and the reduction of acceleration are successfully simulated. The computed pile moment at the pile top considerably exceeds the cracking moment, which can explain the observed damage. The second method is a seismic deformation method. By degrading the interaction spring according to the decrease of effective stress, and by applying the computed ground deformation and the estimated inertial force of the building, a static analysis of the pile is conducted. The computed pile stress exceeds an elastic limit at the pile top and at the border of liquefied layer and non-liquefied layer. This result shows consistency with the observed damage of piles, showing the applicability of this procedure. Through parametric studies, the effect of the degradation of interaction spring on the pile stress is clarified.

KEYWORDS

Hyogoken-Nanbu earthquake; liquefaction; pile foundation; effective stress analysis; elastic-plastic model; seismic deformation method

INTRODUCTION

During the January 17, 1995, Hyogoken-Nanbu Earthquake, a widespread liquefaction on reclaimed land took place and damages to pile foundations were observed. This paper reports the response analysis of a building which suffered a damage to its piles due to liquefaction. Two analytical methods, an effective stress finite element method and a static seismic deformation method, are employed. By comparing the numerical results with the observed damage, the applicability of these numerical methods is examined.

SOIL, BUILDING, AND DAMAGE

The soil profile and the section of the building are shown in Fig. 1. The building is a freezer warehouse built on a reclaimed land in Kobe City. The surface layer of up to -14 m is a reclaimed land by a decomposed weathered granite known as Masado. It overlies the original sea-bed layer of an alluvial clay up to -25 m and an alluvial sand layer up to -34 m . Below it lies a diluvial gravelly sand layer. A prestressed concrete pile with a diameter of 40 cm is driven to -35 m to be supported on the diluvial gravelly sand layer. The building is a steel structure with an elevated first floor by 60 cm above the ground surface. The top part of the pile, up to 1.0 m below the ground surface, is strengthened by a reinforced concrete column of 80 x 80 cm^2 (called foundation column).

After the earthquake, sand boils were observed around the building, indicating that liquefaction took place on this site. A survey of the pile damage performed by excavating the soil around the top part of the piles revealed flexural cracks on several piles. The location of the cracks, with the maximum width of about 1 mm , is approximately 30 cm below the end of the foundation column. Some fracture of concrete along the cracks were observed. A typical damage is depicted in Photo 1. The directionality of the crack was not clear and the residual displacement of the building was not visible. These facts indicates that the damage to the pile was caused by an oscillatory vibration during the earthquake rather than by a lateral spreading of the ground.
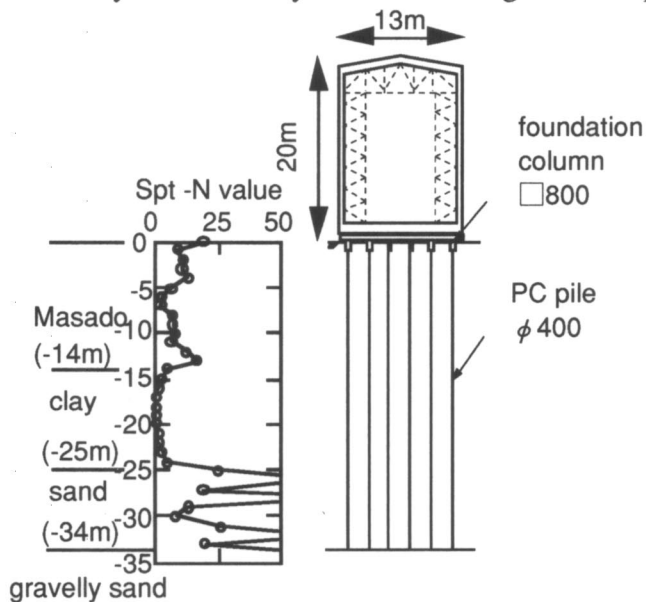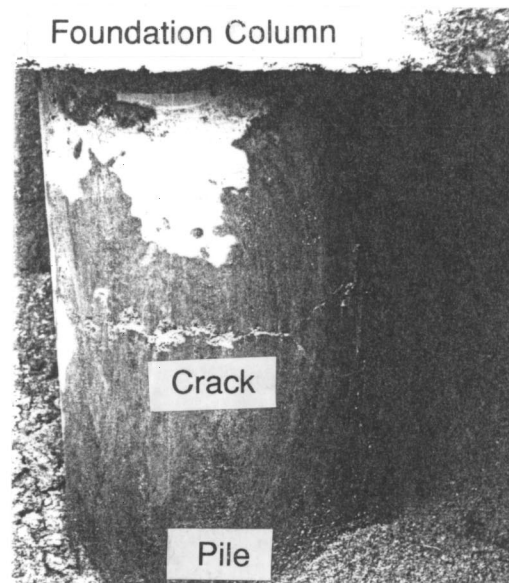

Fig. 1. Soil and structure

Photo 1. Typical damage to pile

EFFECTIVE STRESS FINITE ELEMENT ANALYSIS

Analysis of soil column

The two phase effective stress finite element analysis code, DIANA-J, together with an elastic-plastic constitutive model, the Stress-Density model (Cubrinovski 1993) , is used. Figure 2 shows the numerical model and the assumed soil properties. The soil up to -34 m is modeled by 16 plane strain elements. The surface 8 elements up to - 14m, which are potentially liquefiable soil, are modeled by the Stress-Density model. An analysis of the Port Island vertical array has been conducted with the same numerical technique (Cubrinovski and Ishihara 1996), and the numerical result precisely simulated the observed acceleration records. Since the soil profile of this site is very similar to that of the vertical array site, the parameters of the Stress-Density model applied to the simulation of the vertical array records are used in the present analysis. The liquefaction strength curve represented by the model is compared with the results from cyclic undrained triaxial tests on Masado (Nagase *et al.*, 1995) in Fig. 3.

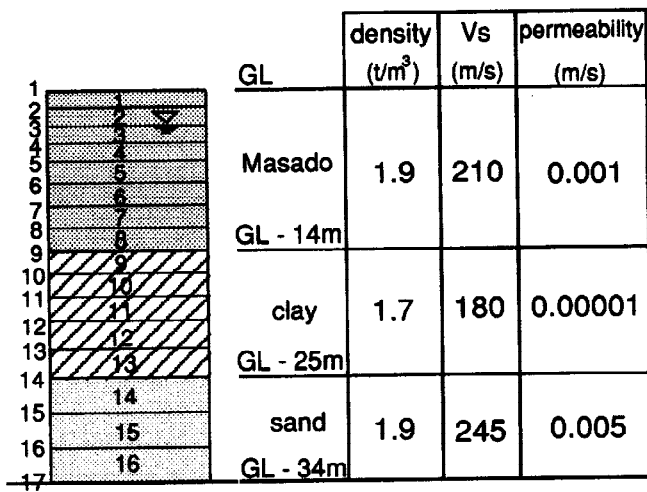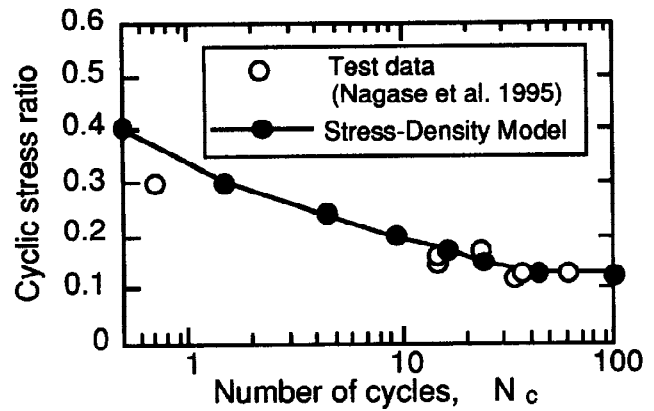| GL	density (t/m³)	Vs (m/s)	permeability (m/s)
Masado GL - 14m	1.9	210	0.001
clay GL - 25m	1.7	180	0.00001
sand GL - 34m	1.9	245	0.005

Fig. 2. Numerical model

Fig. 3. Liquefaction strength curve

The alluvial clay and the alluvial sand are modeled as linear materials with degraded stiffness which has been identified by an equivalent linear analysis of the soil column, prior to the effective stress analysis. The bottom of the model has a fixed condition, and the right and the left boundary are specified to share same displacement in the horizontal and vertical directions. The input acceleration, shown in Fig. 4, is the NS component of the Port Island vertical array record at -32 m. The time increment in the computation is 0.005 seconds. The response acceleration, displacement at the ground surface, and the pore pressure ratio at the sixth layer are shown in Fig. 4. The pore pressure starts to build-up at 3.5 seconds when the excitation intensifies, and the pore pressure ratio reaches 1.0 at around 5 seconds, indicating the occurrence of liquefaction. The pore pressure build-up is similar throughout the Masado layer, and the layers between -4.5 m and -14 m liquefied. The time history of the ground surface acceleration shows an elongation of the period and a reduction in the amplitude following the initiation of liquefaction.
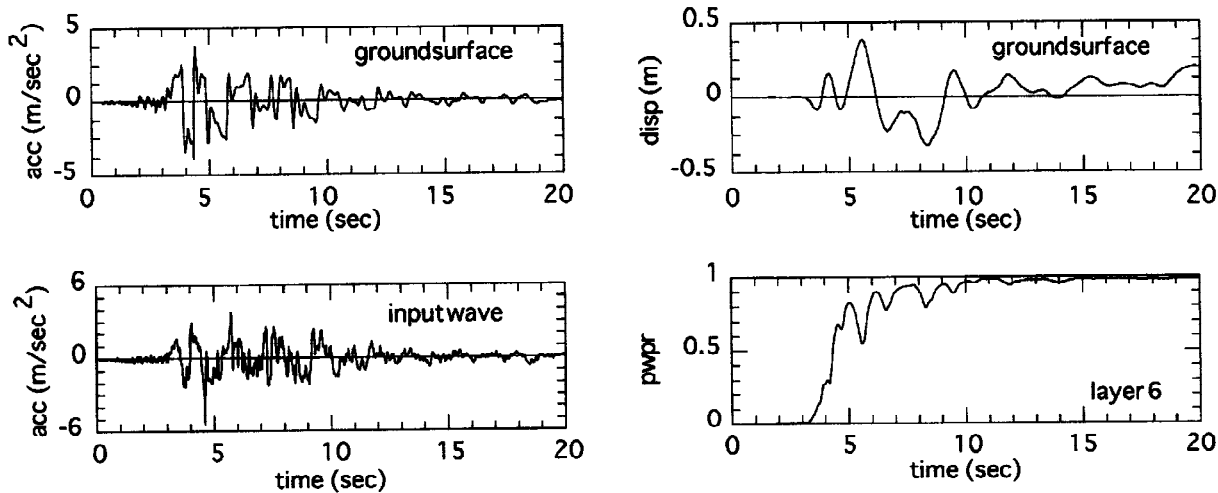

Fig.4. Numerical results of soil column analysis

Figure 5 depicts the distribution of the maximum responses. In the alluvial clay and the alluvial sand layer, the maximum acceleration is nearly constant at the level of the input motion of 5.44 m/sec². In the Masado layer, however, the maximum acceleration decreases because of the liquefaction, resulting in a reduced maximum acceleration of 3.80 m/sec² at the ground surface. The horizontal displacement is amplified in the fifth to the eighth layer where the soil completely liquefied, resulting in a large displacement of 38.2 cm at the ground surface.
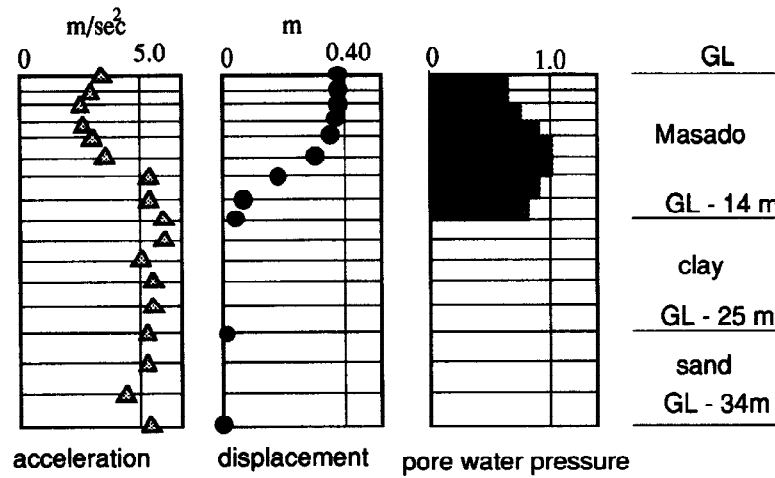
Fig. 5. Maximum response

The effective stress path and the shear stress-strain curve of the sixth layer are plotted in Fig. 6. The effective stress path shows a reduction in the effective stress along in the course of cyclic loading and eventually exhibits cyclic mobility. A reduction in the stiffness associated with the increase in the shear strain and a large shear strain of over 5 % are represented in the numerical result.

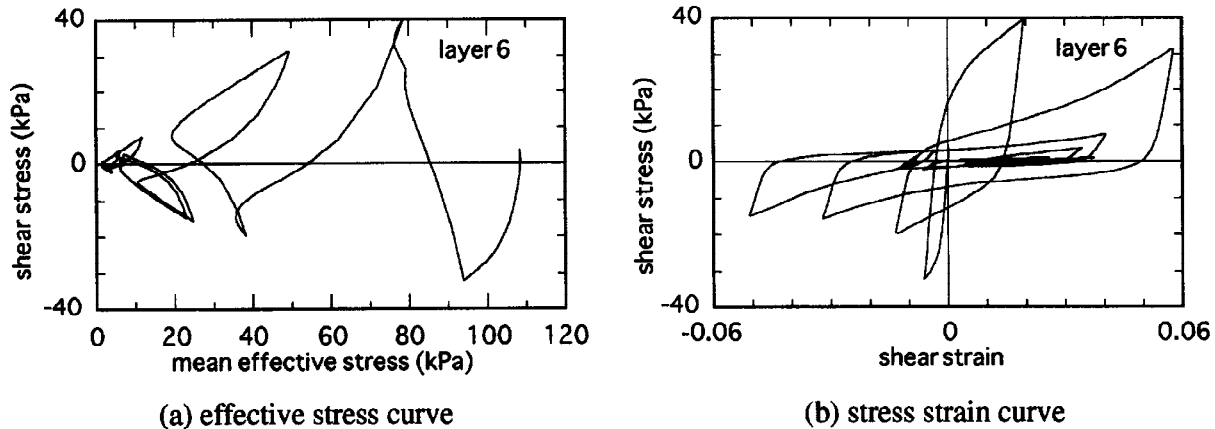(a) effective stress curve

(b) stress strain curve

Fig. 6. Response of soil

Effective stress analysis of soil-pile-building model

The numerical model is described in Fig. 7. The soil stratification and the parameters of the soil are identical to the analysis of the soil column model. The prestressed concrete piles and foundations are modeled by linear elastic beam elements with a damping of 3 % and the building is modeled by linear elastic beam elements with a damping of 1 %. The boundary condition, the input motion, and the computational time increment are the same to those of the soil column analysis.

The time histories of accelerations and displacements at the ground surface, and pore pressure ratios at the fourth layer are plotted in Fig. 8. No significant difference in the accelerations and in the displacements at three different locations (underneath the building, on side of the pile, and in the far field) is observed. This is because the interaction effect is not large since the foundation is not very stiff and the mass of the building is not very large. An oscillation is observed in the pore pressure time history on the side of the pile, which is due to the stress transfer between the soil and the pile. The pile modeled by a beam element in the 2D analysis has the same effect of a continuous wall in terms of the interaction to the adjacent soil. Though this type of modeling is a common practice in the computation at present, it may be necessary to check the effect of the modeling of a pile on the liquefaction and the resulting soil behavior.
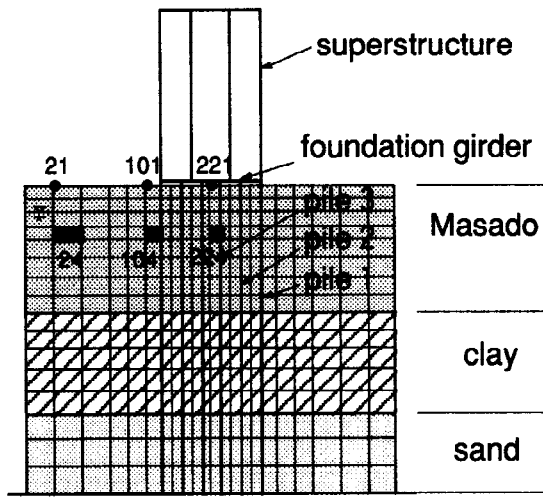
Fig. 7. Numerical model of soil-pile-building system

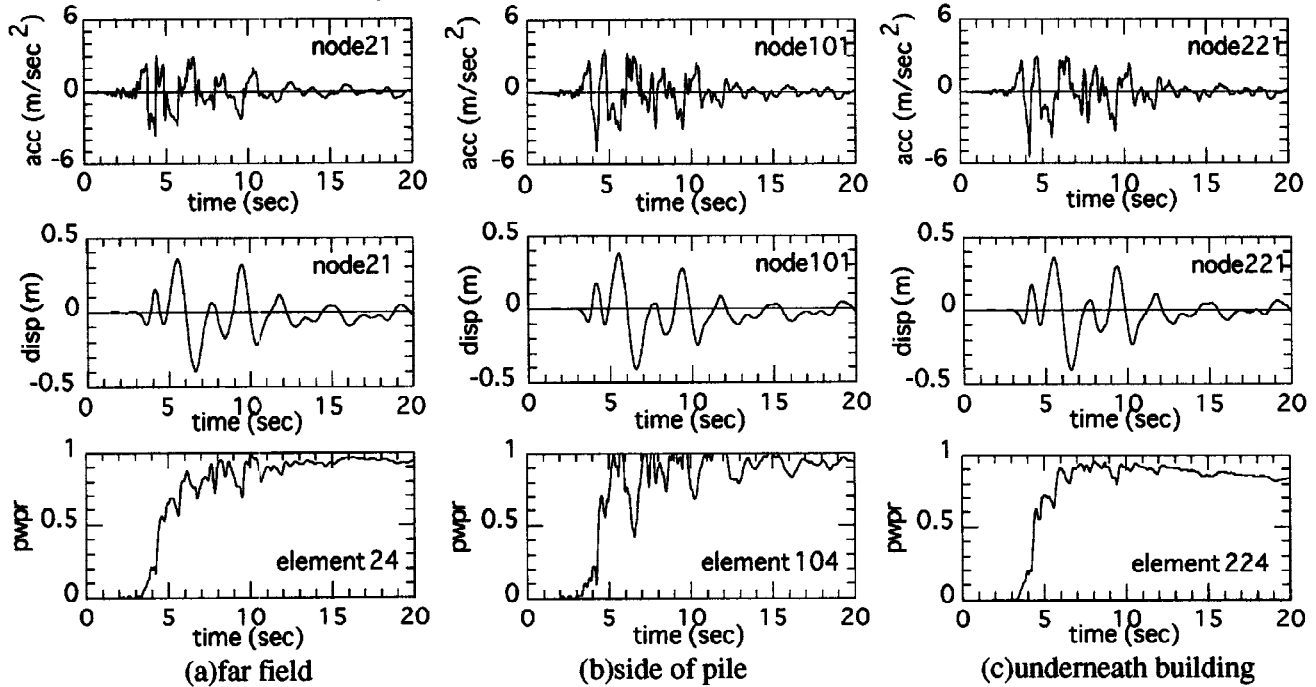(a)far field   (b)side of pile   (c)underneath building

Fig. 8. Time histories of acceleration, displacement, and pore pressure ratio.
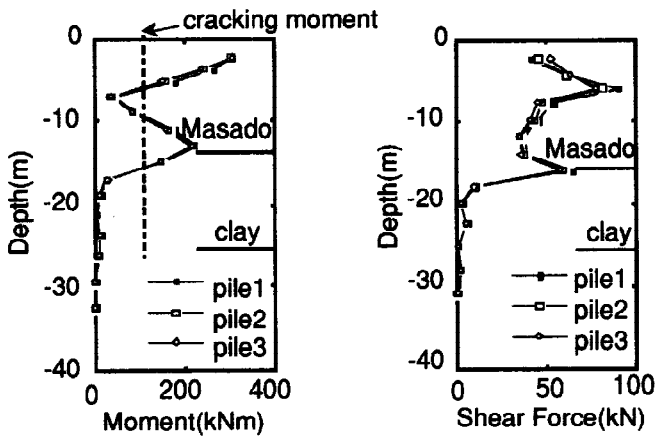
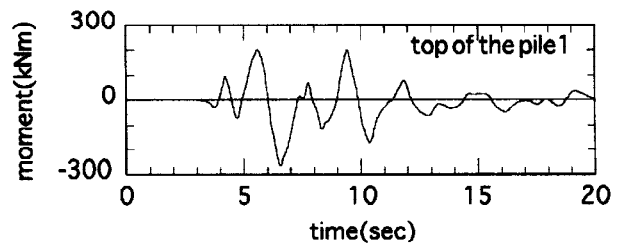

Fig. 9. Maximum stresses along pile

Fig. 10. Time history of bending moment at pile top

The distribution of the maximum bending moments and shear forces are shown in Fig. 9. The bending moment has peak values at the pile top and at the bottom of the Masado layer. The peak bending moments considerably exceed the cracking moment, showing the consistency with the observed damage. The computed bending moment, however, might be overestimated because the pile is modeled as a linear elastic material. No significant difference in the bending moments and the shear forces of the pile 1, pile 2, and pile 3 is observed. The time history of the bending moment at the top of the pile 1, is plotted in Fig. 10. The time history shows clear similarity to the ground displacement, shown in Fig. 8. These facts indicate that the stress of the pile is governed mainly by the ground deformation.

STRESS ANALYSIS OF PILE BY SEISMIC DEFORMATION METHOD

By using the ground deformation, the ground surface acceleration, and the pore pressure in the soil obtained by the effective stress finite element analysis of the soil column, a static stress analysis of a single pile is conducted. Figure 11 shows the numerical model which includes a pile, a foundation column, and a foundation girder. The computation is done for the time when the ground surface displacement takes the maximum value at 5.6 second. The foundation column and the foundation girder are modeled by linear elastic beams. The non-linearity of the flexural stiffness of the pile is considered. The moment-curvature relation of the pile is shown in Fig. 12.
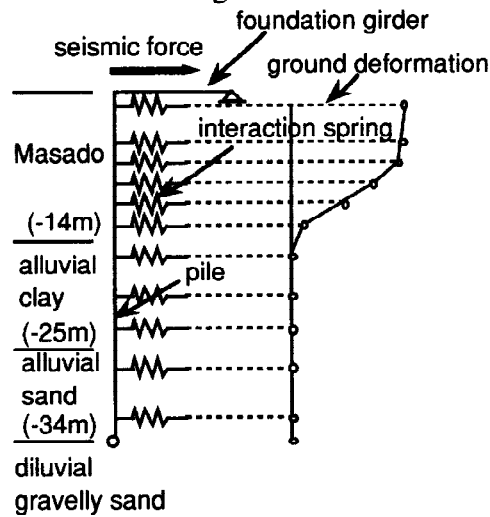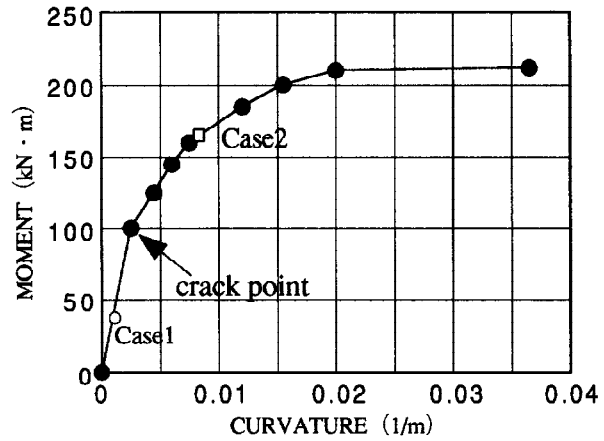

Fig. 11. Numerical model

Fig. 12. Moment-curvature relation of pile

A Winkler type soil-pile interaction spring is assumed. The spring value is determined in the following way;

(1)An initial value, which is commonly used as the value for 1 cm deformation of the spring, is determined by using the following equation.

$$K_{h0} = 0.8 \ E_0 \ (B)^{-3/4} \qquad (1)$$

where E_0 is a ground deformation coefficient in kgf/cm^2 and B is the diameter of the pile in cm.

(2)To incorporate non-linearity in terms of the deformation of the spring, it is assumed that the spring value is proportional to the square root of the spring deformation.

$$K_h = K_{h0} \ (\ y \ )^{1/2} \qquad (2)$$

where y is the spring deformation in cm.

(3)To degrade the spring value in terms of liquefaction, it is assumed that the spring value is proportional to m power of the effective stress.

$$K_h' = K_h (p / p_0)^m \qquad\qquad (3)$$

where p and p_0 are the effective stress at the considered time and at the beginning respectively, and m is a constant. Usually $m = 0.5$ is used to consider the effect of the effective stress on the stiffness of the soil. In a recent experimental study (Lie *et al.* 1995), however, it is reported that $m = 1$ is more appropriate to explain the effect of the liquefaction on the interaction spring. In this analysis, both $m = 0.5$ and $m = 1.0$ are used and the results are compared.

Figure 13 shows the force-deformation relation of the interaction spring determined as above. At the time considered, the pore pressure ratio between -6 m and - 12 m exceeds 0.9.

The inertial force and the ground deformation are applied. The inertia force is computed by multiplying the mass of the building by the acceleration at the ground surface computed in the effective stress analysis of the soil column. The distribution of the ground deformation is shown in Fig. 11, and the numerical cases are described in Table 1. The effect of the constant m, the contribution of the inertial force and the ground deformation on the pile stress, as well as the non-linearity of the pile, are examined.
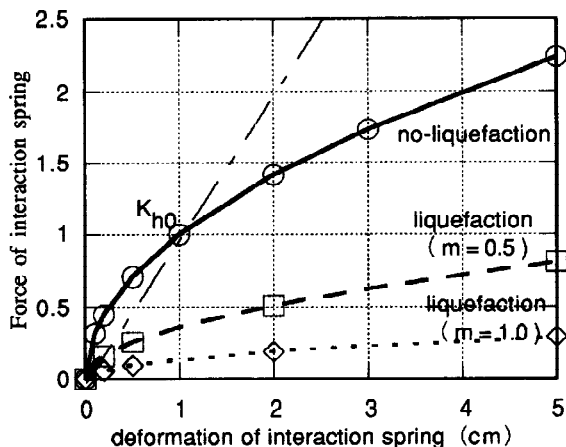

Fig. 13. Force-deformation of interaction spring

Table 1   Numerical Cases

	coefficient"m" degradation of interaction spring	modeling of pile	seismic force	ground deformation
Case1	0.5	non-linear	O	O
Case2	1.0	non-linear	O	O
Case3	0.5	non-linear	O	-
Case4	0.5	non-linear	-	O
Case5	0.5	linear	O	O

The distribution of bending moments along with the pile for Case 1 and Case 2 is shown in Fig. 14. The bending moment takes large values at the pile top and at the bottom of the Masado layer, which is similar to the observation in the finite element analysis. The bending moment at the pile top for Case 2, with $m=1.0$, is larger then the corresponding value for Case 1, with $m=0.5$, showing that the effect of the degradation of the interaction spring on the numerical result is significant. The moment at the pile top plotted on the moment-curvature relation in Fig. 12, indicates that the moment in Case 1 is smaller than the cracking moment while the moment in Case 2 reaches between the cracking and yielding moment. Recalling the observed damage of a large bending crack at the pile top, it can be concluded that Case 2 offers more reasonable numerical result. Figure 15 compares the contribution of the inertial force and the ground deformation to the pile bending moment. The bending moment induced by the inertial force of the building is relatively small and the effect is limited to the very shallow area, while the moment caused by the ground deformation is large especially deep in the ground. Figure 16 compares the bending moment of Case 5 in which the pile is modeled by a linear elastic beam ,with that of Case 1 in which the flexural non-linearity is considered. The bending moment in Case 5 is nearly double of that in Case 1, indicating that a linear modeling overestimates the pile stress.
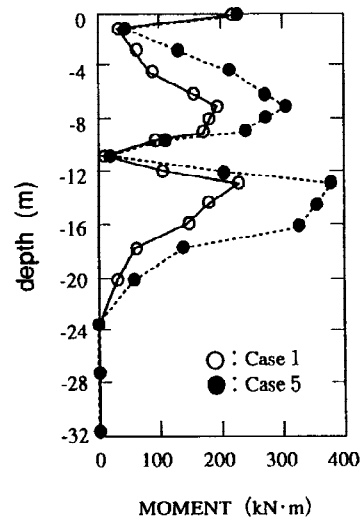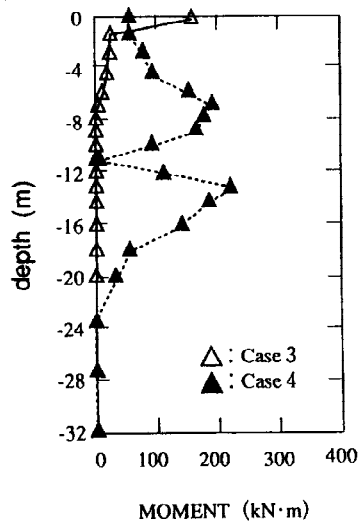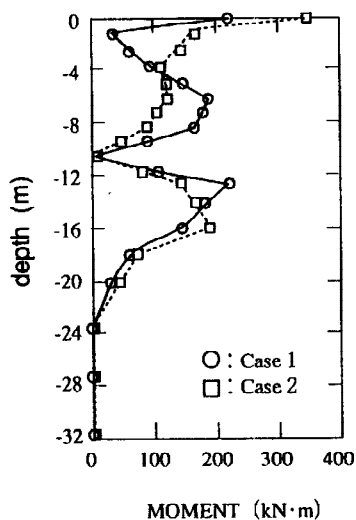
Fig. 14. Maximum moment   Fig. 15. Contribution of external force   Fig. 16. Effect of pile non-linearity

SUMMARY

A response analysis of a pile foundation which was damaged due to liquefaction during the Hyogoken-Nanbu Earthquake is conducted by two numerical methods; an effective stress analysis of soil-pile-building model and a static seismic deformation method. The effective stress analysis successfully reproduces the occurrence of the liquefaction, the resulting stiffness degradation, and a large horizontal displacement. The computed pile stress exceeds the elastic limit, showing that the current method can predict the damage of piles during liquefaction. For further study, the appropriateness of modeling of piles by beam elements in 2D analysis needs to be verified. In a static stress analysis of a pile using the seismic deformation method, the numerical result is affected by the degradation of the interaction spring. The degradation of the spring proportional to the effective stress ($m = 1$) offers a closer result to the observation. The contribution of the ground deformation on the pile stress is very large and it should be considered in the design of piles in a liquefiable ground.

ACKNOWLEDGMENTS

REFERENCES

Cubrinovski, M. (1993). A constitutive model for sandy soils based on a stress-dependent density parameter. Dr. Eng. Thesis, University of Tokyo.

Cubrinovski, M. and Ishihara, K. (1996). Assessment of the Kobe Port Island liquefaction through analytical simulation of the vertical array records. Proc. JSCE Special Conference on the Great Hanshin-Awaji Earthquake Disaster, Tokyo.

L. Lie, et al.(1995), Effect of liquefaction on lateral response of piles by centrifuge model tests, NCEER Bulletin, Vol. 19, Number 1.

Nagase, H. , Shinji, R., Tsujino, S., and Kimura, K.(1995). Liquefaction strength of overconsolidated undisturbed sandy soil samples. Proc. JSSME Annual Meeting, No.30, 1995